Using point cloud registration to mitigate systematic errors in permanent laser scanning-based landslide monitoring

Yihui YANG[1,*], **Daniel CZERWONKA-SCHRÖDER**[2], **Philipp SEUFERT**[1], and **Christoph HOLST**[1]

[1] *Chair of Engineering Geodesy, TUM School of Engineering and Design, Technical University of Munich, Arcisstraße 21, 80333 Munich, Germany, (yihui.yang@tum.de, philipp.seufert@tum.de, christoph.holst@tum.de)*

[2] *Department of Geodesy, Bochum University of Applied Sciences, Am Hochschulcampus 1, 44801 Bochum, Germany, (Daniel.Czerwonka-Schroeder@hs-bochum.de)*

[*] *corresponding author*

Abstract

Permanent laser scanning technology has been utilized for continuous monitoring of natural hazards over the past decade, owing to its ability to capture high spatio-temporal resolution point cloud time series, termed 4D point clouds (3D space + time). These 4D point clouds from PLS enable the detection of intricate surface changes and deeper insights into Earth's surface processes. However, due to the potential instability of the installation platform and environmental variations, significant systematic errors may occur in the point cloud data across different epochs. In this study, we assume that the dominant systematic shifts cause an approximate rigid-body movement of the entire point cloud surface based on the investigation and analysis of continuous total station measurements. By applying rigid registration to the stable areas, we can optimally align these point clouds and thus mitigate the deviations between scanned surfaces. These deviations can reflect the comprehensive impacts of systematic errors during monitoring, such as changes in scanner position and orientation and refraction effects. Preliminary analyses of systematic errors in PLS are conducted on a dataset from a PLS system installed in Vals Valley (Tyrol, Austria) for monitoring a landslide. The total station measurements and the transformation parameters derived from targetless registration exhibit significant daily periodic patterns. Through robust registration, these centimeter-level systematic errors can be mitigated to the millimeter level without using artificial targets or additional sensors.

Keywords: Permanent laser scanning, total station, uncertainty reduction, atmospheric refraction, targetless registration

1 Introduction

Natural hazards such as landslides pose significant threats to infrastructure, ecosystems, and human safety, making continuous and accurate monitoring essential for risk assessment and early warning (Alcántara-Ayala, 2025). Permanent laser scanning (PLS), as the station-fixed and continuous operation of terrestrial laser scanning (TLS), has emerged as a powerful tool for landslide monitoring, offering higher spatial and temporal resolution compared to traditional monitoring methods like total station and GNSS (Czerwonka-Schröder, 2023). Unlike epoch-wise surveys, PLS enables near-real-time observation, capturing subtle surface deformation processes that might be overlooked by conventional methods (Anders et al., 2019). The ability to acquire dense point cloud time series facilitates improved deformation analyses and supports early warning systems in landslide monitoring.

Despite the advantages of PLS in geomonitoring tasks, unexpected (systematic and random) errors may occur in the laser scans during a long-term measurement. While random uncertainties can be typically attenuated by multiple measurements or local averaging, the detection and mitigation of systematic errors remain a challenge. The direct consequence is the occurrence of surface differences between 4D point clouds obtained by PLS in addition to the actual deformations (Kuschnerus et al., 2021). For example, two-epoch scans are not aligned in stable areas due to slight movements of the scanner. Besides, significant diurnal temperature variations or inhomogeneous air densities in the alpine areas may cause changes in distance measurements and laser deflection, resulting in distortions between 4D point clouds (Kuschnerus et al., 2021; Vos et al., 2020). These systematic errors are prone to be regarded as surface changes, leading to incorrect decision-making. Therefore, these errors appearing in PLS should be mitigated before conducting a deformation analysis.

Possible systematic errors occurring in 4D point clouds from PLS are mainly caused by (Kuschnerus et al., 2021):

- Uncalibrated instruments
- Unstable monitoring platform
- Atmospheric refraction effect
- Scanned surface properties.

The final systematic errors presented in the acquired 4D point clouds result from the combined effects of these error sources. Modeling these errors individually and accurately is quite challenging and often requires other sensor data, such as the pose information of the monitoring platform by GNSS and inclination sensors, and sufficient meteorological data in the monitored area. These are difficult to achieve in most applications. For example, placing enough meteorological sensors along the path of the laser beam is impractical.

In most PLS-based landslide monitoring, if the instruments are accurately calibrated and operate stably during the monitoring period, then we assume that the dominant systematic errors in the observations come from the instability (e.g., tilts and movements) of the monitoring platform and atmospheric refraction (e.g., distance variation and ray bending). Supposing that both the platform and atmospheric conditions are constant during a single scan, the platform changes between epochs result only in rigid-body movements between point clouds, which can be represented by a set of transformation parameters (i.e., one transformation matrix). The refraction effect, on the other hand, is related to the change of meteorological parameters (e.g., temperature, air pressure and humidity), as well as to the measuring distance and the geometry of monitored surfaces. Atmospheric refraction mainly affects the speed and path of laser propagation in a systematic way (Friedli, 2020). Some studies calculate the refraction correction by numerical simulation, which effectively improved the observation accuracy (Friedli et al., 2019; Kermarrec et al., 2025). However, simplified models lacking sufficient and real-time meteorological parameters are limited to describe the variable atmospheric conditions in the mountain areas (Zhou et al., 2021).

Since it is difficult to model the refraction-induced errors individually from the observations, empirical analysis and approximation are adopted in this study to mitigate their comprehensive impacts on the raw measurements. For this reason, we deploy a high-precision total station to continuously observe several fixed targets distributed in the monitoring areas, allowing us to investigate the spatio-temporal characteristics of systematic errors.

As mentioned before, the uncertainties caused by the platform's instability can be described by a rigid transformation. If the influence of refraction on the measurement area is similar (i.e., these errors can be approximated as a consistent shift on the scanned surface), then these deviations can be described by similar translation vectors and integrated into the transformation matrix. In other words, the systematic errors in PLS data due to the instability of the instrument platform and refraction effects can be mitigated by rigid point cloud registration.

Based on these basics and assumptions, the main scientific contributions of our study are:

- We intensively analyze continuous measurements (including angles and distances) from a fixed total station beside the laser scanner to infer the influence of platform changes and atmospheric refraction on the captured PLS point clouds.
- Based on the consistent characteristics of the systematic deviations in total station measurements, we apply robust point cloud registration to estimate the optimal transformation of each scan to the reference epoch, aiming to mitigate these systematic errors in PLS data.

2 PLS system and data description

As shown in Fig. 1, a PLS system equipped with a RIEGL VZ-2000i laser scanner was deployed in the Vals Valley (Tyrol, Austria) to continuously monitor a rockfall over several months in 2021, with data acquisition occurring every two hours (Schröder et al., 2023). Several artificial targets (prisms) were fixed in the stable areas surrounding the rockfall surface. A total station (LEICA TM30) was also installed next to the laser scanner to measure the prisms hourly (see Fig. 1d). Both

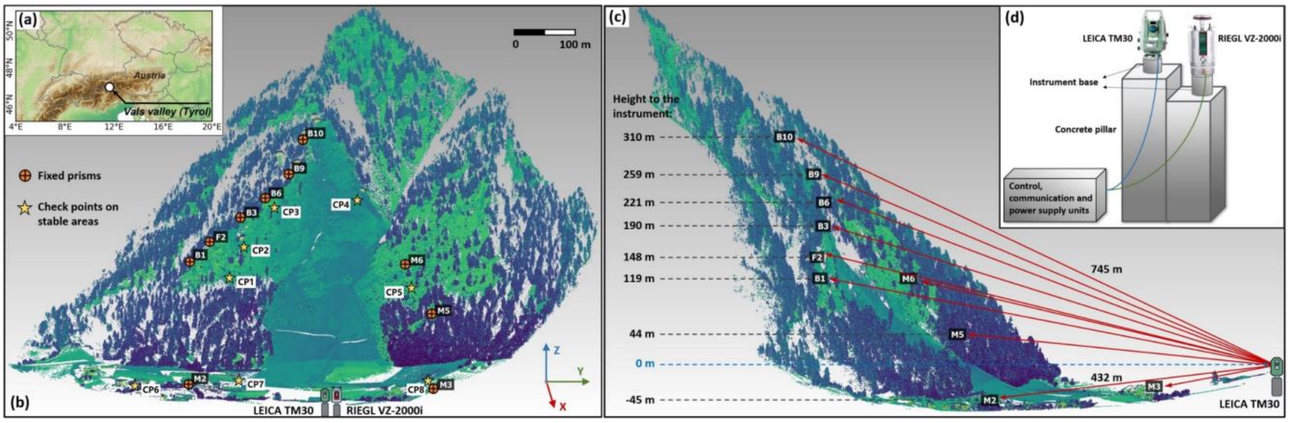

Figure 1. Overview of the rockfall and the monitoring system in the Vals Valley: (a) Location of the rockfall; (b) Captured point cloud and the distribution of prisms and check points; (c) The height and measurement distance of prisms; (d) Setup of the permanent monitoring system.

instruments were installed on a concrete pillar. The inclinometer inside the total station was turned on, thus its angular measurements were corrected by the tilt compensator, yet the tilt compensation was not enabled inside the laser scanner.

As illustrated in Fig. 1b and Fig. 1c, we select ten prisms at different heights and positions, including eight prisms on the rockfall surface (B1, F2, B3, B6, B9, B10, M5 and M6) and two in the valley area (M2 and M3). Besides, we manually define eight check points located on the stable and locally planar surface from the point clouds for evaluating the registration accuracy and mitigation performance, including five points in the upper areas (CP1-5) and three in the valley (CP6-8). The ground in the valley area, although closer to the instruments, generally suffers from stronger temperature variations than the upper rockfall surface, which may lead to more significant refraction effects.

We select six days in May and six days in June to analyze the changes in total station measurements and 4D point clouds from PLS. Due to the data at some epochs being missing or incomplete, the six days selected in May are not continuous. However, data within each day is continuous so that the daily trend of measurements can be presented.

3 Investigation and analysis of total station measurements

To analyze the spatial and temporal trends in the angle and distance measurements of the total station over the monitored area, we examine changes in the measurements of ten prisms located at different positions over the selected 12 days. The temporal trends at the same location as well as the spatial differences in measurement changes between prisms at the same time are evaluated to assess the consistency of systematic errors across the monitored areas.

3.1 Analysis of raw measurements of the total station

Fig. 2 presents the changes in total station measurements at four prisms (relative to the first epoch at 00:00h on May 14th), including horizontal and vertical angles and distances. Prism M2 is located on the valley floor, M6 is located halfway up the rockfall, B1 is close in height to M6 but at a different horizontal angle (see Fig. 1b), and B10 is located at the highest position, with a height difference of 310 m from the instrument.

Fig. 2 shows a clear daily periodicity in the distance measurements across all four prisms, with highly consistent trends at the four locations. The daily variations range between 5-10 mm, with the shortest distance values occurring in the early afternoon, coinciding with peak temperatures. This is because higher temperatures increase the propagation speed of electromagnetic waves. Similarly, from June 11th onward, the average daily temperature rise led to a gradual decrease in overall distance values.

The angle measurements generally exhibit higher noise levels compared to the distance measurements. Vertical angle changes display some degree of daily periodicity, particularly at M2 in the valley, though this pattern is less pronounced at the higher location B10. Interestingly, the vertical angle variations at M6 and B1, which are at the same elevation but have different horizontal angles, show strong similarity. Horizontal angles at all locations tend to increase throughout June, whereas vertical angles show no significant upward or downward trend in this period.

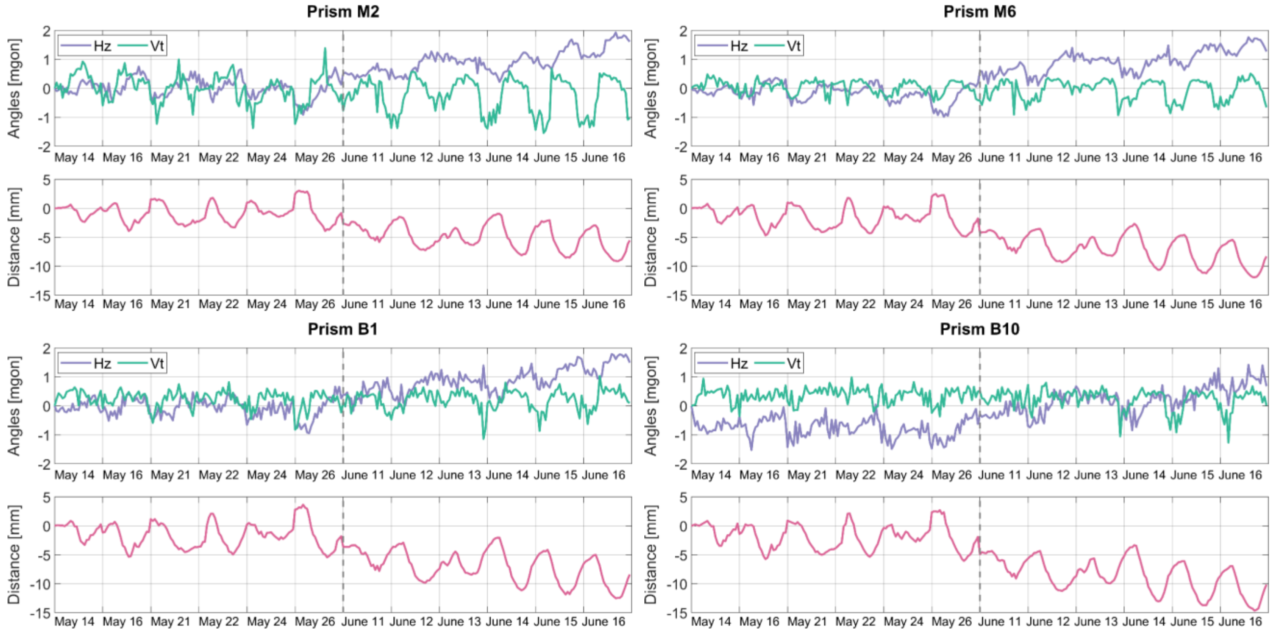

Figure 2. Angle and distance measurements (relative to 00:00h on May 14th) of total station at four prisms.

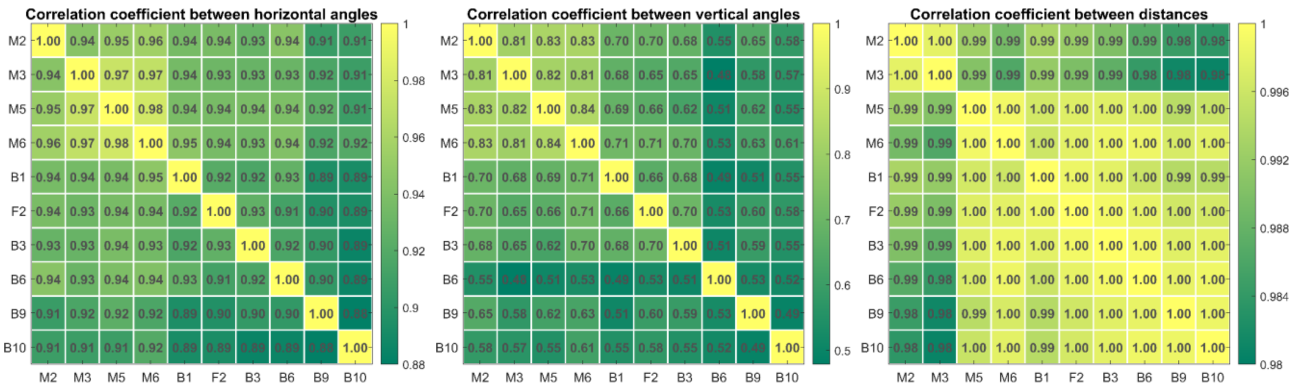

Figure 3. Correlation coefficients between angle and distance measurements at different prisms.

To further evaluate the consistency of angle and distance measurements across different locations, we calculate the correlation coefficients of these measurements between different prisms based on the sequences, as presented in Fig. 3 (with increasing height from M2 to B10). The distance and horizontal angle measurements exhibit strong correlations across all prisms, with all coefficients exceeding 0.88, regardless of height differences. This strong correlation, also evident in the trends in Fig. 2, indicates the potential consistency of systematic errors in distance and horizontal angle measurements within the scanned area.

For vertical angles, strong correlations are observed at lower heights. For instance, the correlation between any two prism measurements exceeds 0.65 for locations below prism F2. However, at higher elevations, the correlation of vertical angles decreases significantly, likely due to varying refraction effects (i.e., differences in the degree of laser beam bending) at different heights.

Aside from the weak correlation of vertical angles in cases of large height differences, the strong correlations among other measurements can be attributed to the similarity of systematic errors in measurements taken at different locations. These errors are primarily caused by the platform tilt and movement that are not fully corrected by the internal compensator in the total station, as well as the consistent refraction effects within a small range, resulting in similar ranging and angular offsets.

3.2 Analysis of spatial differences in total station measurements

To quantify the differences in systematic errors at various locations, we calculate the differences in horizontal angle, vertical angle, and distance measurements between each pair of prisms at the same measuring time, followed by averaging these differences over the 12 days, as shown in Fig. 4. The average differences in horizontal and vertical angle measurements among these prisms are all within 1 mgon. Notably, the average difference in horizontal angles is within 0.5 mgon for all prisms, except for B10 at the highest position.

In general, larger height differences between prisms correspond to greater differences in horizontal angle changes, while prisms at similar heights but different horizontal positions show minimal differences in the horizontal angle measurements. For example, the horizontal angle difference between M6 and B1 is only 0.17 mgon. The spatial distribution of differences in vertical angle measurements appears more random. With the exception of B6, the vertical angle differences at other prisms are mostly within 0.6 mgon.

Except for the prisms in the valley (M2 and M3), the average difference in distance measurements remains within 1.3 mm, with differences in the upper areas below 0.5 mm. This is likely due to the significantly higher variations of the near-surface temperature in the valley, leading to greater differences in distance measurements compared to the upper areas.

In summary, while the systematic errors contained in the angle and distance measurements of the total station vary slightly between different locations, these differences are relatively minor in this landslide monitoring case. Given that the measurement distances are less than 1 km, the positional shifts caused by angular differences are negligible. As a result, the systematic errors across the monitored areas can be considered highly consistent.

To analyze spatial differences in measurement changes over short durations, we also calculate the differences in hourly changes of angle and distance measurements between different prisms. Fig. 5 illustrates the differences in hourly changes of total station measurements between the three upper prisms (M6, B1, B10) and the lowest prism (M2). As shown, while minor variations exist in the differences at the three height levels, the majority of angular differences remain within 1 mgon, and distance differences are within 1 mm. Additionally, the frequency distribution of these differences follows a normal distribution with a zero mean, indicating that these small differences are likely due to random measurement errors rather than systematic ones. This further confirms a high degree of consistency in the systematic deviations of measurements across different locations.

3.3 Analysis of transformation parameters derived by targets

By analyzing the variations in angle and distance measurements from the total station at different locations, we find a high degree of spatial consistency in systematic errors over short time periods. Based on this observation, we assume that the relative positions between these fixed prisms remain invariant. Using their coordinate sequences measured by the total station, we calculate the transformation parameters from each epoch to the reference epoch (00:00h on May 14th), as illustrated in Fig. 6 (where R_x, R_y and R_z represent the rotation angles, and t_x, t_y and t_z represent the

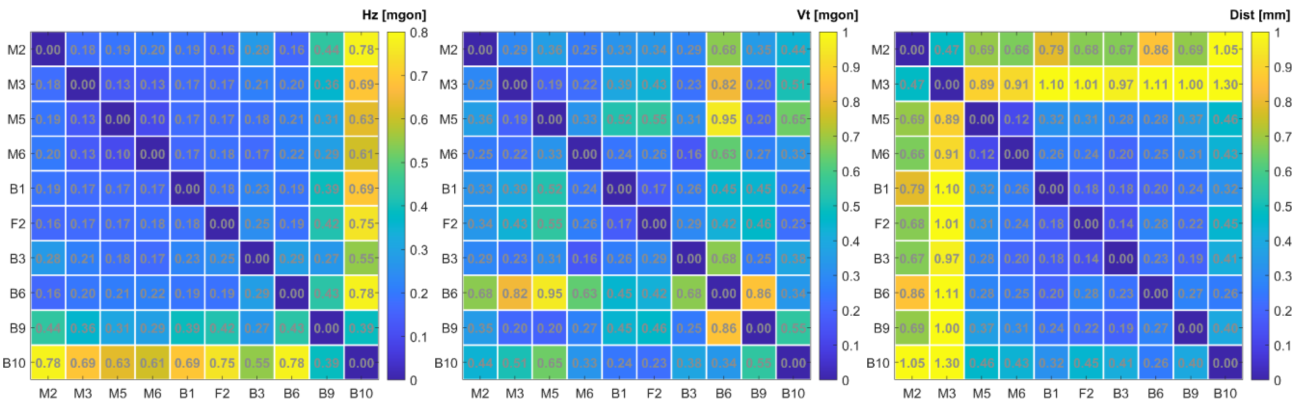

Figure 4. Difference in the mean of measurement sequences (relative to 00:00h on May 14th) between different prisms during the selected period (*Hz*: horizontal angle; *Vt*: vertical angle; *Dist*: distance).

translation components along the three axes). The source and temporal patterns of existing systematic errors are further analyzed based on the variations in the estimated transformation parameters.

(a) Difference between Prism M6 and M2

(b) Difference between Prism B1 and M2

(c) Difference between Prism B10 and M2

Figure 5. Difference in the hourly changes of measurement sequences between M2 and the other three prisms (*Hz*: horizontal angle; *Vt*: vertical angle; *Dist*: distance).

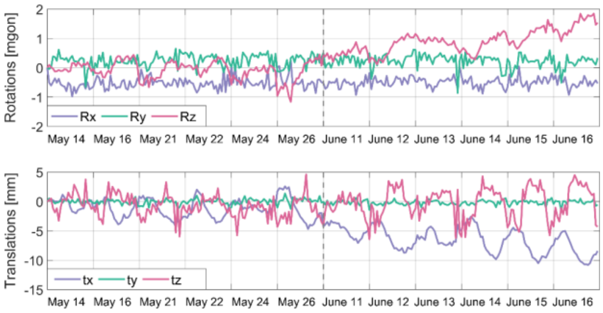

Figure 6. Transformation parameters derived by total station measurements.

In the series of transformation parameters, the rotation angle along the *z*-axis (R_z) shows a significant upward trend in June, while the other two rotation angles remain within ±1 mgon, displaying no daily periodicity or trend. Considering the measurement trends in Fig. 2, we infer that the change in R_z here is due to the change of horizontal angle measurements of the total station.

Compared to the rotation angles, the translation parameters exhibit more pronounced trends. While t_y remains nearly constant, both t_x and t_z show clear daily periodicity. Since the instrument's *x*-axis basically points toward the prism areas, the t_x variation generally follows the distance measurement trends of the total station. Similarly, the trend of t_z corresponds to the changes in vertical angles (as seen in Fig. 2), reflecting the influence of vertical angle variations on the *z*-coordinates of measured prisms.

These observations suggest that most of the instrument platform's tilts are corrected by the tilt compensator in the total station, which can only adjust the inclinations along horizontal axes. The remaining changes (systematic errors) primarily result from a combination of refraction effects and potential platform’s motions (including translations and the rotation around vertical).

4 Rigid registration of 4D point clouds

Since the high similarity of systematic errors has been demonstrated through the analysis of total station measurements in this landslide monitoring case, the 4D point clouds captured at different epochs can be approximated as rigid bodies. This allows systematic errors to be mitigated by optimally aligning the point clouds to a reference epoch. Such an empirical approach reduces the influence of systematic errors on observations without requiring explicit modeling of platform movements or atmospheric refraction effects.

4.1 Targetless registration method

In many landslide scenarios, installing sufficient artificial targets for georeferencing purpose is difficult. Hence, targetless registration algorithms are necessary for processing the acquired 4D point clouds. Given the potential for surface deformation during the monitoring process, it is crucial to identify and use the stable areas for rigid registration. To achieve this, we utilize a robust registration pipeline developed by Yang and Schwieger (2023), along with its extended 4D version (Yang et al., 2024), to compute the time series of transformation parameters. Further details on the specific algorithms can be found in the cited literature.

4.2 Analysis of transformation parameters by rigid registration

Fig. 7 illustrates the estimated transformation parameters between each epoch scan and the reference epoch scan. In the transformation sequence derived from point cloud registration, the translation components exhibit relatively random variations without a clear trend, while the rotation angles — apart from R_z — demonstrate a distinct daily periodicity. This periodicity in rotation is likely attributed to the tilt of the scanner platform, as the scanner did not enable the internal tilt compensation. The observed translation changes represent residual deviations not fully corrected by rotation adjustment. These deviations include the effects of atmospheric refraction and small platform movements. Unlike the transformation parameters derived from total station measurements, where tilt-induced deviations are largely corrected by the internal compensator, the systematic errors in point clouds caused by refraction are reflected in both rotation and translation components.

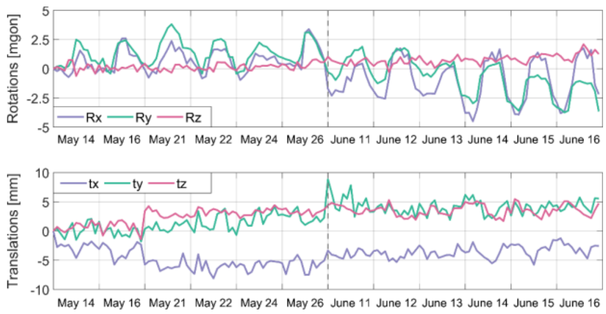

Figure 7. Transformation parameters derived by 4D point cloud registration.

4.3 Evaluation of registration accuracy

The reduction of systematic errors can be reflected by the accuracy of the point cloud registration. To assess the registration accuracy of the applied targetless registration method on 4D point clouds, we calculate the M3C2 (normal) distances (Lague et al., 2013) at the eight check points between the reference and registered scans. Fig. 8 presents the normal distances between one epoch scan and the reference epoch scan before and after registration.

Before registration, the entire point cloud surface exhibits noticeable deviations relative to the reference epoch, with a mean shift of 1.5 cm. The deviations are particularly apparent on the right side of the scan, where distances reach approx. 4 cm. After robust registration, these systematic errors are significantly reduced. The mean normal distance is nearly zero, and most of the distances across the point cloud surface fall within 1 cm, demonstrating the effectiveness of the registration strategy in mitigating systematic errors.

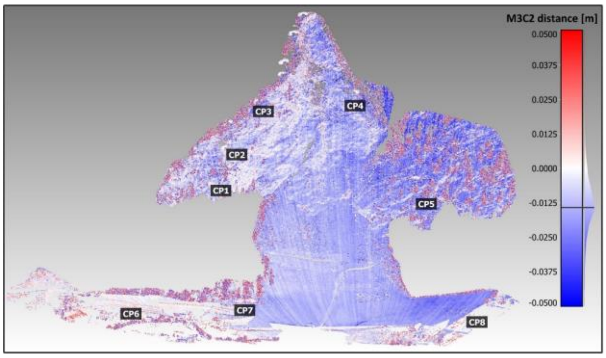

(a) Without registration

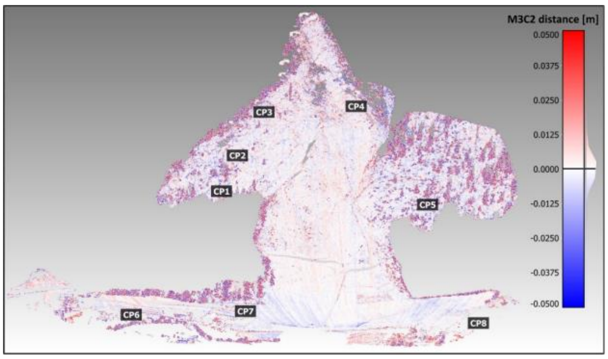

(b) After robust registration

Figure 8. Comparison of M3C2 distances between the scanned surface at one epoch (13:00 on May 16th) and the reference-epoch scan.

To compare the deviations at check points in 4D point clouds, Fig. 9 presents the 12-day trends of normal distances in the upper areas and the valley area, both before and after registration, along with a comparison of their respective averages.

The distances at check points in the upper areas are significantly reduced after registration, particularly during the afternoon when temperatures are highest. The average distances in the upper areas are reduced by nearly 2 mm compared to those before registration. However, due to the strong refraction effects in the valley, systematic errors in the point clouds slightly differ between the valley area and the rockfall surface. Since the rigid registration is applied to the entire region, and the valley area contains far fewer points than the upper area, the aligned point clouds exhibit slightly larger deviations in the lower valley area compared to the upper area. This explains why, in May, the distances in the valley area increase after registration in Fig. 9. Nonetheless, these differences are minimal, averaging approximately 1 mm. Therefore, the analysis of the check point distances indicates that systematic errors in PLS data can be reduced to the millimeter level through point cloud registration in this landslide monitoring scenario.

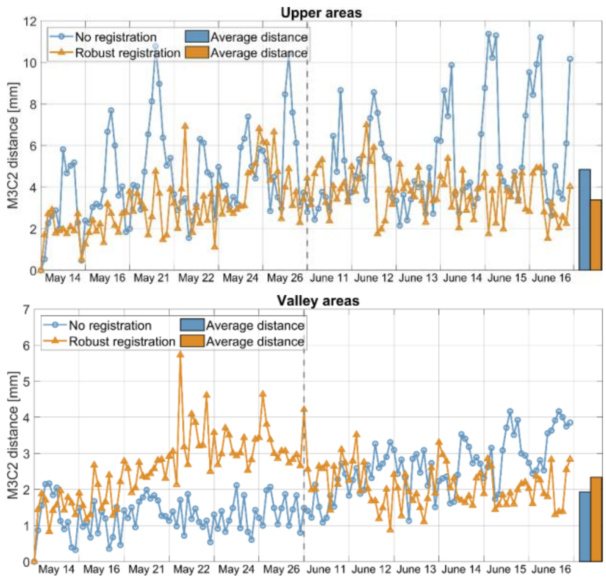

Figure 9. Comparison of M3C2 distances at the check points in the upper areas (CP1–CP5) and the valley (CP6–CP8).

5 Conclusions

This contribution addresses the mitigation of systematic errors in PLS data, primarily arising from the instrument platform instability and atmospheric refraction effects. Based on the analysis of continuous total station measurements, we approximate the influence of systematic deviations as rigid-body movements of the point cloud surface. By applying robust point cloud registration to stable areas, we estimate optimal transformations to align 4D point clouds across different epochs, thus effectively reducing the influence of comprehensive systematic errors. The proposed registration-based mitigation strategy is applied to a PLS dataset from the Vals Valley landslide monitoring site. Results demonstrate that systematic errors with daily periodic patterns can be reduced from several centimeters to the millimeter level without requiring additional artificial targets or auxiliary data collection.

Future work should prioritize the exclusion of areas with strong refraction effects, such as valley regions, by developing adaptive point cloud segmentation methods. Furthermore, leveraging the shifts detected from total station measurements could provide additional corrections for the point clouds. Achieving this would require a denser and more uniformly distributed network of artificial targets, as well as synchronization between the total station and the scanner.

Acknowledgements

This research was partly funded by Federal Ministry of Education and Research (BMBF) as part of the funding measure "Digital GreenTech - Environmental Technology Meets Digitalization" under the funding code 02WDG1696, and partly funded by German Research Foundation (DFG) under grant number 490989047, DFG FOR 5455.

References

Alcántara-Ayala, I. (2025). Landslides in a changing world. *Landslides*, 1-15.

Anders, K., Lindenbergh, R. C., Vos, S. E., Mara, H., De Vries, S., and Höfle, B. (2019). High-frequency 3D geomorphic observation using hourly terrestrial laser scanning data of a sandy beach. *ISPRS Ann. Photogram. Remote Sens. Spat. Inf. Sci.*, 4, 317-324.

Czerwonka-Schröder, D. (2023). Konzeption einer qualitätsgesicherten Implementierung eines Echtzeitassistenzsystems basierend auf einem terrestrischen Long Range Laserscanner. *Ph.D. Thesis*. Technische Universität Bergakademie Freiberg, Freiberg, Germany.

Friedli, E. (2020). Point cloud registration and mitigation of refraction effects for geomonitoring using long-range terrestrial laser scanning. *Ph.D. Thesis*. ETH Zurich, Zurich, Switzerland.

Friedli, E., Presl, R., and Wieser, A. (2019). Influence of atmospheric refraction on terrestrial laser scanning at long range. In: *Proceedings of the 4th Joint International Symposium on Deformation Monitoring (JISDM 2019)*. Athens, Greece.

Kermarrec, G., Sühring, M., and Al-Younis, W. (2025). Impacts of atmospheric turbulence on optic measurements over heterogeneous flat terrain: insights from large eddy simulations. *Optics Express*, 33(2), 3522-3542.

Kuschnerus, M., Schröder, D., and Lindenbergh, R. (2021). Environmental influences on the stability of a permanently installed laser scanner. *Int. Arch. Photogramm. Remote Sens. Spatial Inf. Sci*., 43, 745-752.

Lague, D., Brodu, N., and Leroux, J. (2013). Accurate 3D comparison of complex topography with terrestrial laser scanner: Application to the Rangitikei canyon (NZ). *ISPRS J. Photogram. Remote Sens.*, 82, 10-26.

Schröder, D., Anders, K., Winiwarter, L., and Wujanz, D. (2023). Permanent terrestrial LiDAR monitoring in mining, natural hazard prevention and infrastructure protection–Chances, risks, and challenges: A case study of a rockfall in Tyrol, Austria. In: *Proceedings of the 5th Joint International Symposium on Deformation Monitoring (JISDM 2022)*. Valencia, Spain.

Vos, S. E., Kuschnerus, M., and Lindenbergh, R. C. (2020). Assessing the error budget for permanent laser scanning in coastal areas. In: *Proceedings of the FIG Working Week*.

Yang, Y., and Schwieger, V. (2023). Supervoxel-based targetless registration and identification of stable areas for deformed point clouds. *Journal of Applied Geodesy*, 17(2):161–170.

Yang, Y., Czerwonka-Schröder, D., and Holst, C. (2024). Piecewise-ICP: Efficient registration of 4D point clouds for geodetic monitoring. *EGU General Assembly 2024*, Vienna, Austria, 14–19.

Zhou, J., Shi, B., Liu, G., and Ju, S. (2021). Accuracy analysis of dam deformation monitoring and correction of refraction with robotic total station. *PLoS One*, 16(5), e0251281.